Journal of Inorganic Biochemistry 136 (2014) 73–80

Contents lists available at ScienceDirect

Journal of Inorganic Biochemistry

journal homepage: www.elsevier.com/locate/jinorgbio

Selective hydrolysis of hen egg white lysozyme at Asp-X peptide bonds promoted by oxomolybdate

Karen Stroobants [a], Phuong Hien Ho [a], Eva Moelants [b], Paul Proost [b], Tatjana N. Parac-Vogt [a,*]

[a] Department of Chemistry, KU Leuven, Belgium
[b] Department of Microbiology and Immunology, KU Leuven, Belgium

ARTICLE INFO

Article history:
Received 12 December 2013
Received in revised form 11 March 2014
Accepted 11 March 2014
Available online 12 April 2014

Keywords:
Oxomolybdate
Hen egg white lysozyme
Hydrolysis
Proteins
Metal complexes
Oxoanions

ABSTRACT

The activity of oxomolybdate(VI) towards hen egg white lysozyme (HEWL) was examined under physiological and slightly acidic pH conditions. Purely hydrolytic cleavage of HEWL in the presence of 10 to 100 mM of oxomolybdate(VI) after incubation at pH 5.0 and 60 °C for 2 to 7 days was observed in SDS-PAGE experiments. Four cleavage sites, which all occurred at Asp-X sequences and included the Asp18-Asn19, Asp48-Gly49, Asp52-Trp53 and Asp101-Gly102 peptide bonds, were identified with Edman degradation. The molecular interaction between $[MoO_4]^{2-}$ and HEWL was studied by circular dichroism (CD) and ^1H-^{15}N heteronuclear single quantum correlation (HSQC) NMR spectroscopy. CD spectroscopy revealed a significant decrease in the α-helical content of HEWL upon addition of oxomolybdate, while ^1H-^{15}N HSQC NMR spectroscopy identified the residues which were most affected upon interaction with $[MoO_4]^{2-}$. ^{95}Mo NMR measurements, performed on oxomolybdate solutions containing HEWL, identified the monomeric $[MoO_4]^{2-}$ form as active species in the hydrolytic reaction. The hydrolysis of the Asp-Gly model peptide in the presence of oxomolybdate(VI) was studied by ^1H NMR, further supporting a hydrolytic mechanism where polarisation of the carbonyl is followed by internal nucleophilic attack on the Asp residue.

1. Introduction

Selective cleavage of peptides and proteins is one of the most required and most important procedures in biochemical and bioengineering practice. Currently, either proteolytic enzymes or chemical agents are used to achieve the peptide bond hydrolysis, however, both have several drawbacks and often lack the required selectivity [1,2]. While non-specific peptidases generate too small fragments for most biochemical techniques, rather large peptides are obtained with costly specific peptidases. In addition, enzymatic proteins can only be used in aqueous solution and tuning of their selectivity is not possible [1]. Chemical agents, which in some cases are used as alternative, also suffer from several shortcomings. The best known agent, CNBr, requires harsh conditions, results in low yields and causes an irreversible alteration of the methionine residue where cleavage takes place [3]. Furthermore, hydrolysis leads to fragments larger than the optimal size for most biomedical practices. Therefore, the development of reagents that selectively cleave proteins under mild conditions is still considered as a big challenge [1]. Since pure organic compounds cannot provide strong attacking groups required for the hydrolysis at neutral pH in aqueous solutions, it has been recognized long ago that the presence of metal ions can significantly increase the efficiency of synthetic proteases [1]. The efficient hydrolytically active agents require a strong Lewis acidity, oxophilicity, a high coordination number and fast ligand exchange kinetics. Since many transition metals meet these requirements, the design and synthesis of transition metal complexes that hydrolyse peptide bonds has become an area of intensive study in recent years. Salts and complexes of Co(III) [4,5], Cu(II) [6,7], Ni(II) [8], Mo(IV) [9], Pd(II) [10], Pt(II) [11], Zn(II) [12] and Zr(IV) [S.J. Shealy, K.B. Grant, Abstracts of Papers of the American Chemical Society, vol. 231, 2006, pp. 133] were shown to hydrolyze peptide bonds in dipeptides, oligopeptides and proteins. The highest selectivity was achieved for Pd(II) and Pt(II) assisted cleavage at X-Ser/Thr/His and Met-X bonds, respectively, however very low pH values were required for these reactions [10,11]. Hydrolysis at physiological pH was observed in a few cases including the cleavage of hen egg white lysozyme (HEWL) by Co(III) salts [4], the hydrolysis of bovine serum albumin and HEWL upon incubation with a Cu(II) complex [7] and the fragmentation of tripeptides in the presence of Cp_2MoCl_2 [9]. While for the former two cases no clear specificity was reported, anchoring of Cp_2MoCl_2 to the thiolate of Cys and consequent promotion of an Mo–OH nucleophilic attack towards the amide carbonyl was proposed in case of the molybdocene induced hydrolysis in short peptides [9]. However, no further studies on proteins were reported and so it is not clear whether a similar mechanism would occur in larger molecules. In general, efficient and selective hydrolysis at physiological pH has rarely been achieved

* Corresponding author.
E-mail address: Tatjana.Vogt@chem.kuleuven.be (T.N. Parac-Vogt).

http://dx.doi.org/10.1016/j.jinorgbio.2014.03.006
0162-0134/

and remains a challenging objective in transition metal based artificial protease design.

Inspired by several reports on the biological role of oxovanadates and oxomolybdates, our group has initiated the study of these complexes as potential hydrolytic agents with reactivity towards relevant biomolecules such as RNA, DNA and proteins. Vanadates were previously shown to inhibit several proteolytic enzymes [13]. Furthermore, the interaction with and photooxidative cleavage of different proteins were reported in the presence of vanadate upon UV irradiation [14–18]. Binding of molybdates to nucleotides [19] and ATP [20] resulted in the hydrolytic cleavage of carbohydride and phosphoanhydride bonds, respectively. Interestingly, antitumor activity [21,22] was reported for both oxovanadate and oxomolybdate complexes. Initial studies of our group have investigated the reactivity of V(V) and Mo(VI) oxoanions towards DNA and RNA model systems such as 4-nitrophenylphosphate (NPP), bis-4-nitrophenylphosphate (BNPP) and 2-hydroxypropyl-4-nitrophenylphosphate (HPNP). Hydrolysis of NPP and BNPP was achieved in the presence of both oxoanions, and the active species were identified to be the polynuclear $[V_{10}O_{28}]^{6-}$ [23] and $[Mo_7O_{24}]^{6-}$ [24,25] clusters. The reaction mechanism was studied in great detail for the latter and incorporation of the substrate into the flexible $[Mo_7O_{24}]^{6-}$ structure was shown to lead to ester bond polarisation and consequent nucleophilic attack by water. Conversion of the active Mo(VI) species to $[P_2Mo_5O_23]^{6-}$ upon reaction prevented catalytic activity [25]. However, catalytic cleavage of HPNP was achieved with the same $[Mo_7O_{24}]^{6-}$ reagent [26] and this substrate was also hydrolyzed in the presence of oxovanadate [27]. These promising results have encouraged us to further investigate the potential of oxovanadate and oxomolybdate as reactive species towards biological model systems and recently we have reported the hydrolysis of serine-containing peptides promoted in the presence of oxovanadate and oxomolybdate anions [28,29]. It was shown that polarisation of the carbonyl group of the residue adjacent to Ser upon binding to the V(V) or Mo(VI) transition metal, respectively, led to peptide bond activation, facilitating an internal attack of the hydroxyl group of the Ser residue. The reaction was proven to be purely hydrolytic in nature, demonstrating the first example of hydrolytic peptide bond cleavage promoted by negatively charged oxoanions. While previously reported hydrolytically active metal-substituted polyoxotungstate reactivities towards proteins were relying on the Lewis acidity of an incorporated metal ion [30,31], the demonstrated reactivity in the current paper originates from the oxomolybdate structure itself.

In this paper we further study the reactivity of oxomolybdate(VI) towards HEWL in order to explore the ability of oxoanions to hydrolyze larger biomolecules. Hydrolysis of HEWL, a protein consisting of 129 amino acids was examined under neutral and slightly acidic pH conditions and the molecular interaction between oxomolybdate(VI) and HEWL was studied by several complementary techniques.

2. Experimental section

HEWL and sodium molybdate were purchased from Acros and used without further purification. The primary structure of HEWL is a single polypeptide chain of 129 amino acids with a molecular mass of approximately 14.3 kDa [32].

^{1}H NMR spectra were recorded on a Bruker Avance 400 (400.13 MHz) spectrometer. Solutions containing HEWL (1 mM) were prepared in D_2O and the pD of the solution was adjusted with DCl/NaOD to achieve a pD value of 5 (based on pD = pH value + 0.41). The sample was measured both at room T and 60 °C after dissolving, heated for 3 days at 60 °C and measured again both at room T and 60 °C.

SDS-PAGE was carried out to visualize the hydrolytic activity. Samples of 1.5 mL containing 1 μg/μL (0.07 mM) of HEWL and 0, 10, 20, 50 and 100 mM of oxomolybdate(VI) were incubated at pH 5.0 or 7.0 and 60 °C in the presence or absence of light. Sample aliquots of 100 μL were taken after 2, 4 and/or 7 days. An OmniPAGE electrophoretic cell was combined with an EV243 power supply (both produced by Consort) at 200 V for 1.5 h. SDS-PAGE gels were stained with silver and an image of each gel was taken with a GelDoc EZ Imager (Bio-Rad).

SDS-PAGE gels were blotted onto a polyvinylidene fluoride (PVDF) membrane, the bands were cut after the membrane was stained, destained and rinsed with water. The bands were subjected to automated NH_2-terminal amino acid sequence analysis [33] (Procise 491 cLC protein sequencer, Applied Biosystems, Foster City, CA) based on the Edman degradation reaction as described in the publication cited above.

^{1}H NMR spectra were recorded on a Bruker Avance 400 (400.13 MHz) spectrometer at 293 K. Samples of 500 μL containing 2 mM of aspartyl-glycine (Asp-Gly) in the absence or presence of 120 mM of oxomolybdate(VI) were incubated at pD 5.0 or 7.0. The pD value was adjusted with DCl and NaOD in D_2O. The pH-meter reading was corrected by the equation: pD = pH + 0.41 [34]. As an internal reference, 0.5 mM of 3-trimethylsilyl-1 propionic acid was used. The samples were measured directly after mixing and at different reaction times, and kept at 60 °C between measurements.

^{95}Mo NMR spectra were recorded on a Bruker Avance 600 (39.110 MHz) spectrometer at 293 K. Samples of 3 mL containing 30 mM of oxomolybdate(VI) in the absence or presence of 1.5 mM HEWL were measured after mixing and adjustment of the pD to a value of 5.0. The pD value was adjusted with DCl and NaOD in D_2O. The pH-meter reading was corrected by the equation: pD = pH + 0.41 [34].

CD (circular dichroism) spectroscopy experiments were performed with a JACSO J-810 spectropolarimeter. Far UV spectra were recorded between 200 and 260 nm at 20 °C by using 1 mm quartz cells. Samples of 3 mL containing 5 μM of HEWL and 0 to 200 μM of oxomolybdate were prepared in acetate buffer (100 mM) at pH 5.0 and measured after mixing.

^{15}N-^{1}H HSQC (heteronuclear single quantum correlation) spectra were recorded on a Bruker Avance 600 (600.13 MHz) spectrometer at 293 K. For the acquisition of the HSQC spectra, 768 scans were collected for each FID, using the 'hsqcetf3gf' pulse programme with 512 data points in the F1 dimension and 3072 data points in the F2 dimension with spectral width of 2128 Hz (^{15}N) and 9615 Hz (^{1}H). Samples of 500 μL containing 1 mM of HEWL in the absence and presence of 4 mM of oxomolybdate(VI) and a pH of 5.2 in 10% D_2O were measured after mixing. The pH value was adjusted with HCl and NaOH.

3. Results and discussion

3.1. Hydrolysis of HEWL promoted by molybdate(VI)

Solutions of 1.0 μg/μL (0.07 mM) of HEWL were incubated with sodium molybdate at pH 5.0 and 60 °C during 2, 4, and 7 days. Since the melting of HEWL was shown to occur only at about 75 °C, the protein structure is expected to be stable at 60 °C [35]. However, to ensure the stability of HEWL at 60 °C and after incubation, ^{1}H NMR spectra of the protein were measured both at room temperature and 60 °C after dissolving at pD 5 as well as incubation at pD 5 and 60 °C during 3 days (Figure S1). Although some temperature effects occurred, the characteristic peaks below 0 ppm which are indicative of protein folding [30], were observed under all mentioned conditions. Therefore, it can be assumed that HEWL is stable at 60 °C, also after incubation during longer periods. The concentrations of oxomolybdate(VI) in the reaction mixtures were ranging from 10 to 100 mM. The SDS-PAGE experiments were carried out after 2, 4, and 7 days and the results are shown in Fig. 1. Two fragments with a molecular mass of ~12 and 9 kDa were observed for all samples containing different concentrations of oxomolybdate(VI). The intensity of these two bands increased with increasing incubation time. The sum of the molecular mass of the two bands is significantly larger than the molecular mass of HEWL (14.3 kDa), suggesting that they result from the cleavage at two specific sites of HEWL. The smaller fragments produced by the cleavage at these two sites should have masses of ca. 2 and 5 kDa, which are too low to detect on SDS-PAGE since they migrate together with the dye front.

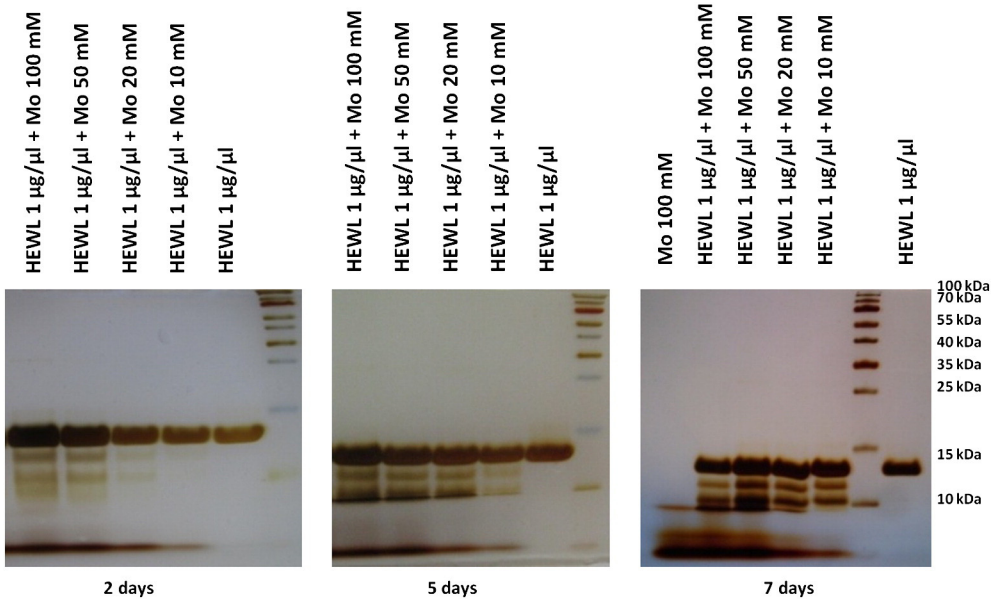

Fig. 1. SDS-PAGE of HEWL. Hydrolysis of 1.0 μg/μL (0.07 mM) of HEWL in the presence of oxomolybdate(VI) (10, 20, 50, and 100 mM) after 2, 5, and 7 days at pH 5.0 and 60 °C.

Interestingly, although the aqueous speciation of oxoanions is highly dependent on the starting concentration of molybdate, the identical cleavage sites observed in all experiments indicate that the same type of oxoanion is the hydrolytically active species in all cases. Hydrolysis of HEWL was also observed in the presence of oxovanadate, however, the reactivity was considerably lower in this case.

The brown bands that appeared at the bottom of the gels were only detected in the samples where oxomolybdate(VI) is present. To test the origin of these bands, a control sample containing only the sodium molybdate solution and no HEWL was used in a similar SDS-PAGE experiment (data not shown). As expected, the brown band also appeared, confirming that these bands do not originate from protein fragments but are due to the presence of molybdate. These are most likely products formed in the reaction between oxomolybdate(VI) and dithiothreitol (DTT) which is present in the sample buffer used for the SDS-PAGE experiments [36].

Solutions of 1.0 μg/μL (0.07 mM) of HEWL were also incubated at pH 7.0 in the presence of oxomolybdate(VI) with concentrations ranging from 10 to 100 mM at 60 °C. SDS-PAGE was carried out after 2 and 7 days as shown in Fig. 2, and interestingly the same fragment with a molecular mass of about 12 kDa was observed. Although a fragment of similar size was observed as in the reaction performed at pH 5.0, the reaction at higher pH appeared to be much slower.

As previous studies have shown that photoradiation of molybdate solutions can result in reduction of oxomolybdate anions and can lead to the formation of reactive species, the effect of visible light radiation was also examined [37–41]. Therefore, solutions of 1.0 μg/μL (0.07 mM) of HEWL were incubated with 20 mM of oxomolybdate(VI) at pH 5.0 and 60 °C and either left in the daylight or kept in the dark. After 2 days, SDS-PAGE was carried out and the results are shown in Fig. 3. As can be seen from the gels, there was no difference between these samples, suggesting that the cleavage of HEWL promoted by oxomolybdate(VI) is not photo-oxidative in nature. Furthermore, the Edman degradation experiments (vide supra) unambiguously proved that the cleavage was hydrolytic in nature. These hydrolytic reactions occur at slower rates as compared to the photo-oxidative cleavage of different proteins in the presence of vanadate, where half lives of only few minutes were obtained for comparable or up to 50 times lower oxometalate/protein ratios [16,42]. However, the cleaved polypeptide fragments resulting from oxidative cleavage are difficult to identify by Edman degradation [16] and in general less useful in biochemical and biomedical procedures which require protein fragmentation.

3.2. Identification of the hydrolysis sites

The peptide fragments resulting from the HEWL hydrolysis in the presence of oxomolybdate(VI), were identified by western blot and subsequent NH_2-terminal Edman degradation analysis of a minimum of 5 residues. Fragments with the LysValPheGlyArg NH_2-terminus of HEWL (at ~12 kDa and <5 kDa) or one of the following NH_2-terminal sequences were obtained: AsnTyrArgGlyTyr (at ~ 12 kDa), GlySerThrAspTrp (at ~ 9 kDa), TrpGlyIleLeuGln (at ~ 9 kDa) and GlyAsnGlyMetAsn (at < 5 kDa). From these results four cleavage sites at the Asp18-Asn19, Asp48-Gly49, Asp52-Trp53 and Asp101-Gly102 peptide bonds were identified. Hydrolysis at these positions results in four pairs of fragments with molecular masses of about 2.0/12.3, 5.4/8.9, 5.8/8.5 and 11.1/3.2 kDa, respectively. These results are in good agreement with the estimated masses of 12 and 9 kDa on the low resolution gels in Fig. 1, as both bands seem to contain two fragments of around 12.3/11.1 and 8.9/8.5 kDa, respectively.

Strikingly, all four cleavage sites in HEWL occurred at an Asp-X amide bond. The previous studies on oxomolybdate(VI) promoted hydrolysis of dipeptides have indicated that the oxoanion has high affinity towards hydrolysis of X-Ser bonds, and interestingly both mechanisms of hydrolysis are characterized by the requirement of side chain assistance in the hydrolysis of the adjacent peptide bond. In the hydrolysis of X-Ser dipeptides, higher reaction rates were observed due to an N → O acyl rearrangement and internal attack on the Mo(VI) polarized carbonyl. Similar internal nucleophilic attack is known in Asp residues, leading to Asp-X peptide bond hydrolysis [43]. Polarisation of the carbonyl in the presence of oxomolybdate(VI) and consequent internal nucleophilic attack can lead to the observed Asp directed hydrolysis as shown in Fig. 4. Polarisation of the carbonyl of the Asp residue might be in competition with coordination to the carboxyl of the Asp side chain in accordance with a proposed interaction between vanadate and phosphoenolpyruvate [44]. However, the latter interaction will not lead to hydrolysis of the peptide bond. Previous studies have shown that the carbonyl coordination hydrolysis mechanism is favoured at pH values below 6.0 and it is in part responsible for the known labile properties of Asp containing

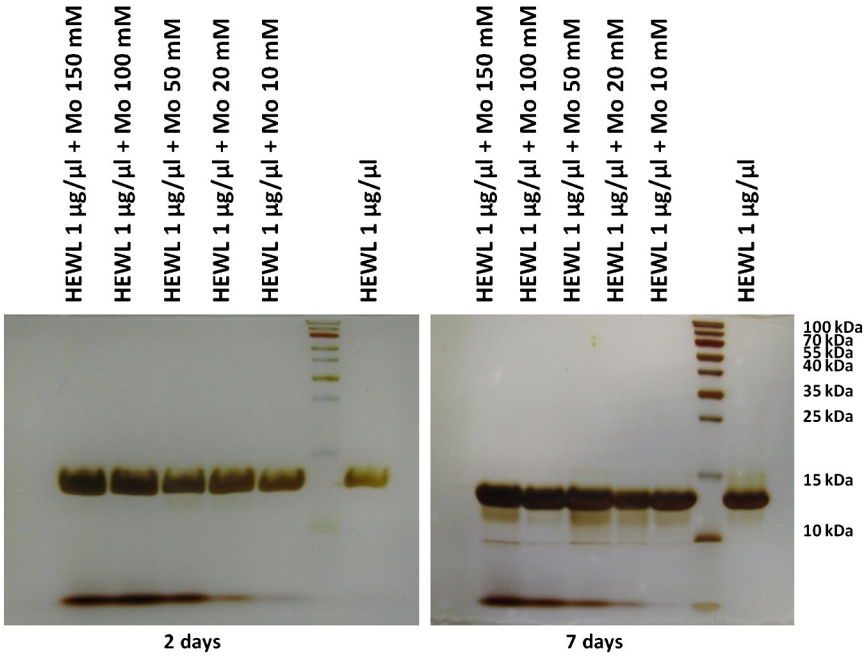

Fig. 2. SDS-PAGE of HEWL. Hydrolysis of 1.0 μg/μL (0.07 mM) of HEWL in the presence of oxomolybdate(VI) (10, 20, 50, 100, and 150 mM) after 2 and 7 days at pH 7.0 and 60 °C.

peptide bonds in acidic media [43]. While peptide bond hydrolysis was shown to be dominant over succinimidyl peptide formation, which also occurs at pH values below 6.0, formation of iso-Asp, D-Asp and D-iso-Asp species are more favourable reactions above pH 6.0 as compared to the peptide bond hydrolysis pathway. The pH dependence of the nucleophilic attack of the Asp side chain on Asp-X peptide bonds can explain the much faster rate of HEWL hydrolysis observed at pH 5.0 as compared to pH 7.0, as well as the low reaction rate which was previously reported for Asp-Ala hydrolysis in the presence of oxomolybdate(VI) at pH 7.0 [28]. Furthermore, the different pH conditions as well as changes in the pKa of side chain residues in proteins might explain the distinct selectivities in dipeptide versus protein targets.

In order to gain more insight into the ability of oxomolybdate(VI) to cleave Asp-X peptide bonds, the hydrolysis of the dipeptide Asp-Gly was investigated at 60 °C and pD 5.0 and 7.0, both in the absence and presence of oxomolybdate(VI). The reactions were conveniently followed by ^{1}H NMR spectroscopy since the peaks corresponding to the CH of the Asp residue in Asp-Gly (~4.25 ppm) as well as the peak corresponding to the free Gly, which is the reaction product (~3.98 ppm), were well separated throughout the reaction. Integration of the proton resonances allowed for calculation of the hydrolysis rate constants at the different conditions, which are presented in Table 1. The labile character of the Asp-Gly bond is reflected by the high degree of background cleavage both at pD 5.0 and 7.0. However, the rate of Asp-Gly hydrolysis at pD 5.0 is increased by 40% upon addition of oxomolybdate(VI), while no enhancement is observed at pD 7.0, which is in agreement with the earlier proposed mechanism. While only 3% hydrolysis of Asp-Ala (2 mM) was reported in the presence of 120 mM of oxomolybdate(VI) at 60 °C and pD 7.0 after 60 h in a previous study [28], 10% conversion of Asp-Gly was observed under the same conditions in the present study. It should be noted in this regard that a considerable influence of the adjacent residue was reported for the rate of Asp-X hydrolysis. The highest conversion rates were observed for Asp-Gly hydrolysis, followed by the peptides Asp-Pro, Asp-His and Asp-Ser [43]. In general, Asp-X bonds are stabilized in the protein structure, as reflected by the fact that protein fragmentation was not detected in the absence of oxomolybdate(VI) while considerable background cleavage was observed for the hydrolysis of Asp-Gly in the absence of oxomolybdate(VI).

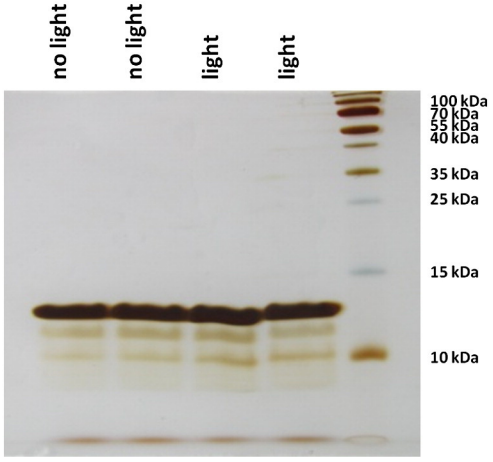

Fig. 3. SDS-PAGE of HEWL. Hydrolysis of 1.0 μg/μL (0.07 mM) of HEWL in the presence of 20 mM of oxomolybdate(VI) after 2 days at pH 5.0 and 60 °C in the absence (lane 1 and 2 — replicas) and presence (lane 3 and 4 — replicas) of light.

Monomeric oxomolybdate was previously identified as the active species in dipeptide bond hydrolysis by detailed kinetic experiments [28]. The monomeric $[MoO_4]^{2-}$ was also shown to coordinate to the tripeptide glycylglycylglycine [45]. In contrary, no studies reporting on peptide or protein interactions with $[Mo_7O_{24}]^{6-}$ are known, and our experiments also do not give evidence for this interaction. The $[Mo_7O_{24}]^{6-}$ has been previously reported to promote phosphodiester bond hydrolysis, a process which occurs via partial detachment of an MoO_4 unit and the incorporation of the structurally analogous phosphoester substrate into the polyoxometalate structure. Due to the lack of any structural resemblance with MoO_4, this process is unlikely to occur with peptides and proteins [28]. However, as the speciation of oxomolybdate anions is highly dependent on temperature, pH and concentration, it is interesting to consider the species distribution under reaction conditions of pH 5.0 and 7.0. In general, high pH and low concentrations of molybdate favour $[MoO_4]^{2-}$ in solution, while low pH and high concentrations favour the formation of polyoxoanions. We have previously developed a thermodynamic model, which allowed us to calculate the percentage

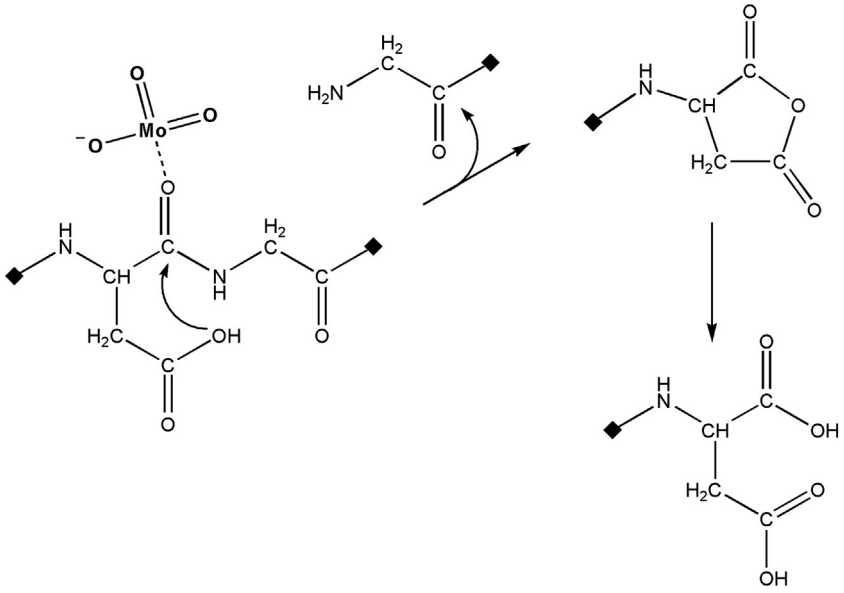

Fig. 4. Schematic representation of the Asp assisted peptide bond hydrolysis in the presence of molybdate(VI).

of different oxomolybdate species, depending on the conditions [24]. The formation constants of the different oxomolybdate species at 50 °C were used to estimate the $[MoO_4]^{2-}$ percentage in 10, 30 and 100 mM solutions at pH 5.0 and 7.0, respectively (Table 2). The calculations reveal that under all conditions the $[MoO_4]^{2-}$ anion is present in solution, although its concentration ranges from ca. 9.8 to 23 mM in 10 to 100 mM solutions, respectively. However, since the HEWL concentrations in the hydrolysis experiments were in the order of 1 μg/μL (0.07 mM), the active $[MoO_4]^{2-}$ species is always in large excess with respect to HEWL. Furthermore, a ^{95}Mo NMR measurement of molybdate(VI) in the presence of HEWL indicates slight shifting and severe broadening of the characteristic $[MoO_4]^{2-}$ peak as shown in Fig. 5 which presumably are caused by interactions with the protein. Similar effects were previously observed for interaction between vanadate and protein molecules. Different vanadate species were observed in ^{51}V NMR and peak shifting, intensity decrease and broadening were observed for two peaks, in accordance with those vanadate species interacting with tubulin [39]. Interestingly, the peaks of the polyoxo forms could not be detected in the ^{95}Mo NMR spectrum of a 30 mM solution either due to the excessive broadening in the presence of HEWL or because the equilibrium between $[MoO_4]^{2-}$ and $[Mo_7O_{24}]^{6-}$ is fully shifted to the $[MoO_4]^{2-}$ form upon addition of HEWL.

3.3. Interactions of oxomolybdate(VI) with HEWL

3.3.1. CD spectroscopy

CD spectroscopy was further used to gain information about the secondary structure of HEWL in solution. The secondary structure content can be determined by CD spectroscopy in the far-UV spectral region as α-helices have two minima at 208 and 222 nm, while β-sheets have a single minimum at 215 nm. CD spectroscopy was previously applied as a method to study POM-protein interactions [46–49].

HEWL mainly consists of α-helices and only contains a small β-plate region, which is reflected in a CD spectrum with minima at 208 and 222 nm, characteristic for α-helical structure content. Solutions containing 5.0 μM of HEWL and varying concentrations of oxomolybdate(VI) (ranging from 0 to 200.0 μM) were prepared in acetate buffer (100 mM) at pH 5.0. As can be seen in Fig. 6, the CD signal intensity gradually decreases upon the addition of increasing amounts of oxomolybdate(VI). The changes in CD spectra suggest that interaction between oxomolybdate(VI) and HEWL takes place in solution which leads to the loss of α-helical structure content of HEWL. In a previous study on the hydrolysis of HEWL in the presence of the heteropolyoxometalate Ce(IV)-Keggin, a similar decrease in α-helical structure content was observed upon addition of 1 equivalent of the polyoxometalate complex. However, as can be seen in Fig. 6, an increase in the oxomolybdate(VI) concentration causes a gradual decrease in the α-helix content indicating multiple electrostatic interactions between oxomolybdate(VI) and the protein. Furthermore, the deformation of the peaks at the largest oxomolybdate(VI) concentrations is indicative of denaturation of the protein.

3.3.2. ^{1}H-^{15}N HSQC

The interaction of oxomolybdate(VI) with HEWL was further examined by ^{1}H-^{15}N HSQC NMR spectroscopy. Measurement of the ^{1}H-^{15}N HSQC spectrum of HEWL in the absence and presence of the oxometalate provides information on the shifting of amino acid residues and thus the positions where interaction with oxomolybdate(VI) takes place. ^{1}H-^{15}N HSQC spectra were recorded on a 1.0 mM HEWL sample in the absence and in the presence of 3.0 mM of Na_2MoO_4. The

Table 1
Asp-Gly hydrolysis rate constants in the absence and presence of oxomolybdate(VI) at pD 5.0 and 7.0 and 60 °C.

Asp-Gly+	pD	k_{obs} (s^{-1})	$t_{1/2}$ (h)
/	5.0	1.68×10^{-6}	114.5
molybdate(VI)	5.0	2.34×10^{-6}	82.3
/	7.0	0.87×10^{-6}	220.4
molybdate(VI)	7.0	0.84×10^{-6}	228.8

Table 2
Molybdate(VI) speciation in 10, 30, and 100 mM solutions at pH 5.0 and 7.0.

	$[MoO_4]^{2-}$ (initial)	$[MoO_4]^{2-}$ (equilibrium)	% $[MoO_4]^{2-}$
pH 5	10 mM	9.8 mM	98%
	30 mM	17 mM	59%
	100 mM	23 mM	23%
pH 7	10 mM	10 mM	100%
	30 mM	30 mM	100%
	100 mM	100 mM	100%

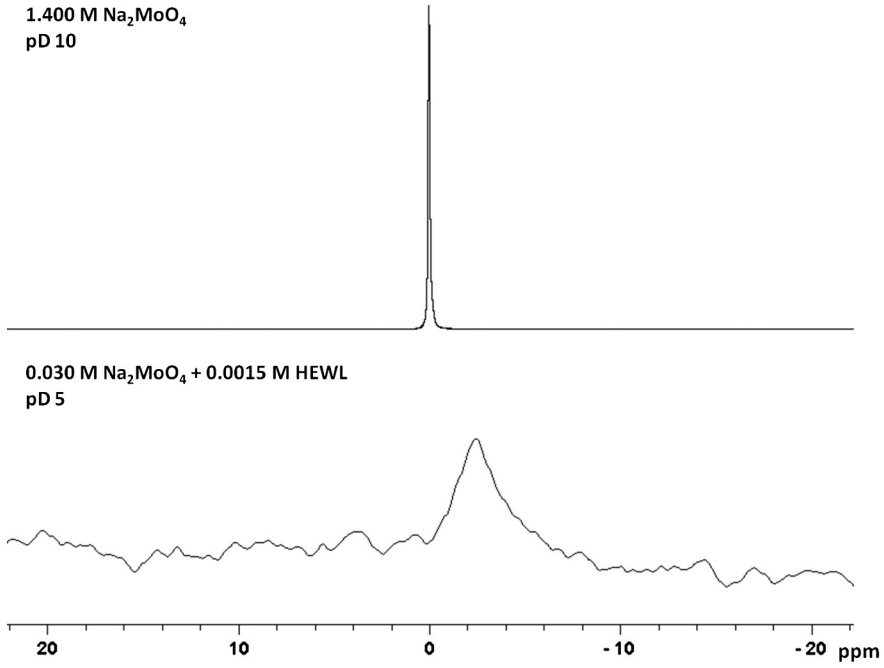

Fig. 5. ^{95}Mo NMR spectrum of 30 mM of oxomolybdate(VI) in the presence of 1.5 mM of HEWL at pD 5.0 (bottom) as compared to a reference spectrum of sodium molybdate at high concentration and pD 10 where only the $[MoO_4]^{2-}$ is expected to be present (top). The shifting and severe broadening of the peak occur due to interactions with the protein.

chemical shift perturbations (CSP) of the measured peaks were calculated by the following equation:

$$\Delta\delta = \sqrt{(\Delta\delta_H)^2 + \frac{(\Delta\delta_N)^2}{25}}$$

where $\Delta\delta_H$ is the difference in the ^{1}H amide resonance before and after ligand addition, while $\Delta\delta_N$ is the ^{15}N difference of the amide resonance before and after ligand addition. $\Delta\delta$ is the chemical shift perturbation (CSP) upon binding of the ligand, oxomolybdate(VI) in this case. The CSP value allows the determination of the relative strength of interaction between an amino acid residue and the ligand (Table 3).

By overlapping the ^{1}H-^{15}N HSQC NMR spectrum of HEWL in the absence of oxomolybdate(VI) with the one recorded in the presence of oxomolybdate(VI), all the shifted peaks could be assigned. Upon visualisation of the observed shifts as well as the hydrolysis sites as shown in Fig. 7, it is obvious that shifts occur at distinct positions as well as in the surroundings of these sites. Small shifts are observed for residues Asp52, Trp53 and Gly102, which are located in the immediate vicinity of the cleaved peptide bonds. No shifting was seen for residues Asp18, Asn19, Asp48, Gly49 and Asp101, however, several side chains surrounding these positions are affected by the addition of oxomolybdate(VI). From these results, higher preference for interaction at the Asp52-Trp53 and Asp101-Gly102 peptide bonds might be expected. In addition to the shifts observed in the vicinity of the cleavage sites, several other shifts were also observed suggesting that only certain interactions can cause peptide bond hydrolysis. Medium to large CSPs were observed for the side chains of most solvent accessible Arg residues. These interactions are most likely electrostatic in nature as they occur between the side chain of Arg residues, containing a positively charged guanidinium group, and the negatively charged molybdate. Although a shift was seen for Ser36, cleavage did not occur at neighbouring peptide bonds as this residue is distant from any of the hydrolysis positions in the 3D HEWL structure. None of the nine remaining Ser residues were shifted. Since two Ser residues, Ser50 and Ser100, are located near the Asp48-Gly49 and Asp52-Trp53 hydrolysis sites, assistance of these residues could be anticipated in accordance with the previously described Ser side chain N → O acyl rearrangement mechanism [28]. However, since no shifting was observed for either of both residues, the proposed Asp side chain assistance mechanism is the most likely to occur also at these positions. Modelling and docking studies are required to gain more detailed understanding of differences in interaction and reaction with dipeptide versus protein targets.

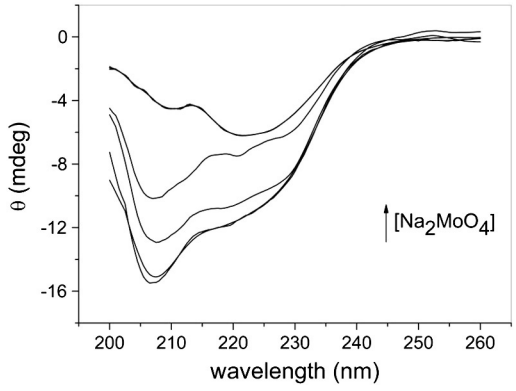

Fig. 6. CD spectra of 5.0 μM of HEWL in the presence of different concentrations of oxomolybdate(VI) (0 → 200.0 μM:bottom→top) in 100 mM acetate buffer at pH 5.0.

3.4. Selectivity of the hydrolysis

The SDS-PAGE and Edman degradation experiments clearly indicated that oxomolybdate selectively hydrolyzes HEWL at four distinct

Table 3
Relationship between CSP (Δδ) and interactions [50].

Δδ	Interaction
<0.015	No
0.015–0.025	Small
0.025–0.05	Medium
>0.05	Large

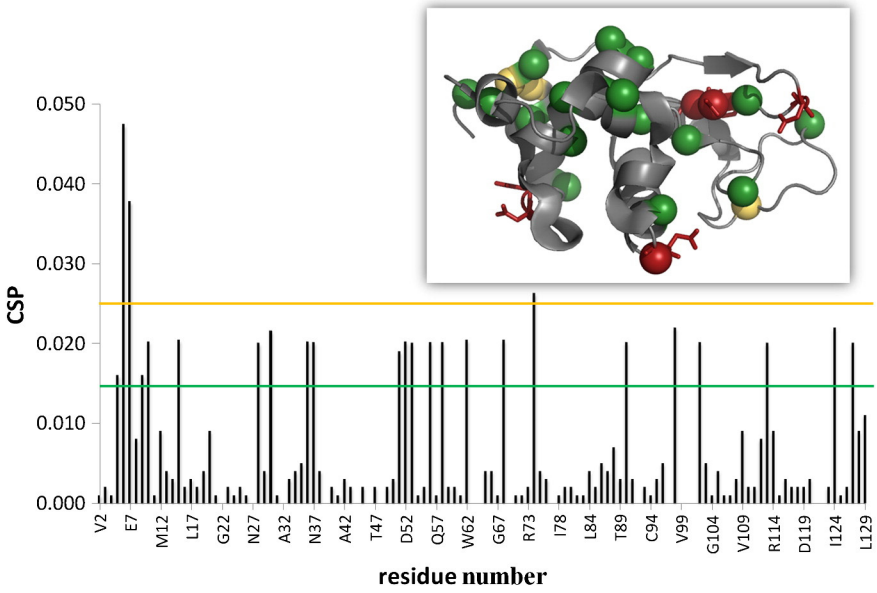

Fig. 7. ^{1}H, ^{15}N HSQC chemical shift perturbations (CSP) for HEWL resonances in the presence of 3 equivalents of oxomolybdate(VI). Shifted residues are schematically represented on the cartoon visualisation of HEWL in the inset (residues with medium shifts as yellow spheres and residues with small shifts as green spheres). The hydrolysis positions are presented in red, small shifts are seen for Asp52, Trp53 and Gly102, these are shown as red spheres.

positions having an Asp-X sequence. Visualisation of the cleavage sites occurring at the Asp18-Asn19, Asp48-Gly49, Asp52-Trp53 and Asp101-Gly102 peptide bonds on the three-dimensional structure of HEWL shows that all four positions are located in solvent accessible loops. The loops containing the Asp18-Asn19 and Asp101-Gly102 peptide bonds are found in the α-helical part of the structure, while the Asp48-Gly49 and Asp52-Trp53 peptide bonds are located near the small β-sheet region of HEWL. Interaction in the α-helical region is clearly evidenced in the CD spectra through the decrease in α-helical structure content upon addition of increasing amounts of oxomolybdate(VI) to the HEWL solution. Furthermore, several shifts in the ^{1}H, ^{15}N HSQC NMR spectra were observed in the α-helical region of HEWL. Although binding effects in the β-sheet part of the structure could not be deduced from the CD spectroscopy data direct shifts of Asp52 and Trp53 were seen in the ^{1}H, ^{15}N HSQC NMR experiments.

While in previous studies with dipeptides, which were performed at neutral pH, Gly-Ser was identified as the most favourable bond to be hydrolyzed in the presence of oxomolybdate(VI), only Asp-X bonds were efficiently hydrolyzed in the reaction with HEWL. In these studies, $[MoO_4]^{2-}$ was identified as the active oxomolybdate(VI) species and although it is not the most abundant species at pH 5.0 at all studied concentrations, it is likely to be the active species also in these protein hydrolysis reactions. The preferential hydrolysis of Asp-X bonds at pH 5.0 presumably is a consequence of the higher labile character of these bonds in acidic conditions. A 100-fold faster cleavage of the Asp-Gly bond compared to other peptide bonds was reported in dilute acids [43]. The interaction of oxomolybdate with the carbonyl oxygen leads to polarisation of the peptide bond thus facilitating the subsequent nucleophilic attack by a hydroxyl group [28]. The importance of oxomolybdate in the hydrolysis mechanism has also been experimentally proven, as for control experiments no hydrolysis was observed either in peptides or in HEWL in the absence of oxomolybdate.

4. Conclusions

In this study we report the first example of purely hydrolytic protein cleavage promoted by an oxomolybdate ion. The cleavage of HEWL was shown to be remarkably selective for Asp-X sequences, and occurred at the Asp18-Asn19, Asp48-Gly49, Asp52-Trp53 and Asp101-Gly102 peptide bonds. Previous studies with dipeptides have shown that oxomolybdate(VI) has high affinity towards the hydrolysis of X-Ser bonds. For both mechanisms side chain assistance and polarisation of the carbonyl bond by oxomolybdate are essential. However, while in the hydrolysis of X-Ser dipeptides, an N → O acyl rearrangement and an internal attack of the Ser side chain hydroxide on the carbon atom of the peptide bond occur, in Asp-X peptide bond hydrolysis an internal attack of the Asp side chain hydroxide on the peptide bond causes formation of a cyclic anhydride with release of the C-terminal peptide and followed by hydrolysis of the anhydride to the N-terminal peptide. The interaction between oxomolybdate and HEWL leads to significant decrease in the α-helical structure content of the protein, consistent with the interaction near the cleavage sites. ^{1}H,^{15}N HSQC NMR spectroscopy measurements revealed that not only residues in the immediate vicinity of the four cleavage sites were affected upon addition of oxomolybdate, but that Arg side chains were also implicated in the binding. The latter interactions are presumably electrostatic in nature and occur between the negatively charged oxomolybdate anion and the positively charged guanidinium group of the Arg side chains. Further experiments, including docking studies, will be needed in order to fully elucidate the mechanism of this novel reaction.

Acknowledgements

K.S. thanks the FWO Flanders (Belgium) for the doctoral fellowship. P. H. H. thanks the Vietnamese Government and KU Leuven for a doctoral fellowship. T. N. P. V. thanks KU Leuven (OT/13/060) and FWO Flanders (G.0864.14 N) for the financial support. P.P. thanks the Concerted Research Actions (G.O.A./2013/014) of the KU Leuven for the support.

Appendix A. Supplementary data

Supplementary data to this article can be found online at http://dx.doi.org/10.1016/j.jinorgbio.2014.03.006.

References

[1] K.B. Grant, M. Kassai, Curr. Org. Chem. 10 (2006) 1035–1049.
[2] J.P. Whitelegge, S.M. Gomez, K.F. Faull (Eds.), Proteomics of Membrane Proteins, Academic Press, 2003.
[3] B.J. Smith (Ed.), Protein Sequencing Protocols, Humana Press, Totowa, 1997.

[4] C.V. Kumar, A. Buranaprapuk, A. Cho, A. Chaudhari, Chem. Commun. (2000) 597–598.
[5] J.W. Jeon, S.J. Son, C.E. Yoo, I.S. Hong, J. Suh, Bioorg. Med. Chem. 11 (2003) 2901–2910.
[6] M.S. Kim, J. Suh, Bull. Korean Chem. Soc. 26 (2005) 1911–1920.
[7] V. Rajendiran, M. Palaniandavar, P. Swaminathan, L. Uma, Inorg. Chem. 46 (2007) 10446–10448.
[8] W. Bal, R.T. Liang, J. Lukszo, S.H. Lee, M. Dizdaroglu, K.S. Kasprzak, Chem. Res. Toxicol. 13 (2000) 616–624.
[9] A. Erxleben, Inorg. Chem. 44 (2005) 1082–1094.
[10] L. Zhu, N.M. Kostic, Inorg. Chim. Acta 339 (2002) 104–110.
[11] N.M. Milovic, L.M. Dutca, N.M. Kostic, Chem. Eur. J. 9 (2003) 5097–5106.
[12] M. Yashiro, Y. Kawakami, J.I. Taya, S. Arai, Y. Fujii, Chem. Commun. (2009) 1544–1546.
[13] D.C. Crans, Pure Appl. Chem. 77 (2005) 1497–1527.
[14] C.R. Cremo, G.T. Long, J.C. Grammer, Biochemistry 29 (1990) 7982–7990.
[15] C.R. Cremo, J.A. Loo, C.G. Edmonds, K.M. Hatlelid, Biochemistry 31 (1992) 491–497.
[16] J.C. Grammer, J.A. Loo, C.G. Edmonds, C.R. Cremo, R.G. Yount, Biochemistry 35 (1996) 15582–15592.
[17] S.M. Hua, G. Inesi, J. Biol. Chem. 275 (2000) 30546–30550.
[18] E.E. Fetsch, A.L. Davidson, Proc. Natl. Acad. Sci. U. S. A. 99 (2002) 9685–9690.
[19] H. Weil-Malherbe, R.H. Green, Biochem. J. 49 (1951) 286–292.
[20] E. Ishikawa, T. Yamase, J. Inorg. Biochem. 100 (2006) 344–350.
[21] A.M. Evangelou, Crit. Rev. Oncol. Hematol. 42 (2002) 249–265.
[22] H. Yanagie, A. Ogata, S. Mitsui, T. Hisa, T. Yamase, M. Eriguchi, Biomed. Pharmacother. 60 (2006) 349–352.
[23] N. Steens, A.M. Ramadan, G. Absillis, T.N. Parac-Vogt, Dalton Trans. 39 (2010) 585–592.
[24] L. Van Lokeren, E. Cartuyvels, G. Absillis, R. Willem, T.N. Parac-Vogt, Chem. Commun. (2008) 2774–2776.
[25] E. Cartuyvels, G. Absillis, T.N. Parac-Vogt, Chem. Commun. (2008) 85–87.
[26] G. Absillis, E. Cartuyvels, R. Van Deun, T.N. Parac-Vogt, J. Am. Chem. Soc. 130 (2008) 17400–17408.
[27] N. Steens, A.M. Ramadan, T.N. Parac-Vogt, Chem. Commun. (2009) 965–967.
[28] P.H. Ho, K. Stroobants, T.N. Parac-Vogt, Inorg. Chem. 50 (2011) 12025–12033 (American Chemical Society).
[29] P.H. Ho, T. Mihaylov, K. Pierloot, T.N. Parac-Vogt, Inorg. Chem. 51 (2012) 8848–8859.
[30] K. Stroobants, E. Moelants, H.G.T. Ly, P. Proost, K. Bartik, T.N. Parac-Vogt, Chem. Eur. J. 19 (2013) 2848–2858.
[31] K. Stroobants, G. Absillis, E. Moelants, P. Proost, T.N. Parac-Vogt, Chem. Eur. J. (2013), http://dx.doi.org/10.1002/chem.201303622.
[32] C.C.F. Blake, D.F. Koenig, G.A. Mair, A.C.T. North, D.C. Phillips, V.R. Sarma, Nature 206 (1965) 757–761.
[33] T. Loos, A. Mortier, P. Proost, in: M.H. Tracy, J.H. Damon (Eds.), Methods in Enzymology, vol. 461, Academic Press, 2009, pp. 3–29.
[34] Covingto Ak, M. Paabo, R.A. Robinson, R.G. Bates, Anal. Chem. 40 (1968) 700.
[35] T. Knubovets, J.J. Osterhout, P.J. Connolly, A.M. Klibanov, Proc. Natl. Acad. Sci. U. S. A. 96 (1999) 1262–1267.
[36] S.J.N. Burgmayer, E.I. Stiefel, Inorg. Chem. 27 (1988) 2518–2521 (American Chemical Society).
[37] C.V. Kumar, A. Buranaprapuk, G.J. Opiteck, M.B. Moyer, S. Jockusch, N.J. Turro, Proc. Natl. Acad. Sci. U. S. A. 95 (1998) 10361–10366.
[38] T. Jyotsna, K. Bandara, C.V. Kumar, Photochem. Photobiol. Sci. 7 (2008) 1531–1539 (The Royal Society of Chemistry).
[39] J.J. Correia, L.D. Lipscomb, J.C. Dabrowiak, N. Isern, J. Zubieta, Arch. Biochem. Biophys. 309 (1994) 94–104.
[40] J.C. Grammer, J.A. Loo, C.G. Edmonds, C.R. Cremo, R.G. Yount, Biochemistry 35 (1996) 15582–15592 (American Chemical Society).
[41] G. Zhang, B. Keita, C.T. Craescu, S. Miron, P. de Oliveira, L. Nadjo, J. Phys. Chem. B 111 (2007) 11253–11259 (American Chemical Society).
[42] C.M. Bergamini, M. Signorini, S. Hanau, M. Rippa, P.P. Delaureto, M.A. Cremonini, Arch. Biochem. Biophys. 321 (1995) 1–5.
[43] B. Testa, J.M. Mayer (Eds.), Hydrolysis in Drug and Prodrug Metabolism, Wiley-VCH, Weinheim, 2003.
[44] M. Aureliano, J. Leta, V.M.C. Madeira, L. Demeis, Biochem. Biophys. Res. Commun. 201 (1994) 155–159.
[45] T. Yamase, M. Inoue, H. Naruke, K. Fukaya, Chem. Lett. (1999) 563–564.
[46] G. Zhang, B. Keita, J.-C. Brochon, P. de Oliveira, L. Nadjo, C.T. Craescu, S. Miron, J. Phys. Chem. B 111 (2007) 1809–1814 (American Chemical Society).
[47] G. Zhang, B. Keita, C.T. Craescu, S. Miron, P. de Oliveira, L. Nadjo, Biomacromolecules 9 (2008) 812–817 (American Chemical Society).
[48] L. Zheng, Y. Ma, G. Zhang, J. Yao, B.S. Bassil, U. Kortz, B. Keita, P. de Oliveira, L. Nadjo, C.T. Craescu, S. Miron, Eur. J. Inorg. Chem. 2009 (2009) 5189–5193 (WILEY-VCH Verlag).
[49] L. Zheng, Y. Ma, G. Zhang, J. Yao, B. Keita, L. Nadjo, Phys. Chem. Chem. Phys. 12 (2010) 1299–1304 (The Royal Society of Chemistry).
[50] A.S. Kanai, A, Y. Fukuda, K. Okada, T. Matsuda, T. Sakamoto, Y. Muto, S. Yokoyama, G. Kawai, M. Tomita, RNA 15 (2009) 420–431.